Journal of NeuroVirology, 13: 130–138, 2007

ISSN: 1355-0284 print / 1538-2443 online
DOI: 10.1080/13550280601187185

informa
healthcare

West Nile virus encephalitis: sequential histopathological and immunological events in a murine model of infection

David Garcia-Tapia,[1,2] Daniel E Hassett,[1] William J Mitchell Jr,[2] Gayle C Johnson,[2] and Steven B Kleiboeker[1]

[1]*Department of Veterinary Pathobiology Department, University of Missouri–Columbia, and* [2]*Veterinary Medicine Diagnostic Laboratory, College of Veterinary Medicine, University of Missouri–Columbia, Columbia, Missouri, USA*

West Nile virus (WNV) has emerged as an important cause of encephalitis in humans and horses in North America. Although there is significant knowledge about the pathogenesis of disease caused by this flavivirus and about the immunity against it, no reports exist describing the sequence of pathological changes and their correlation to the immune response in the brain following infection with WNV. In this report the authors describe the major histopathological changes, as well as changes in cytokine and chemokine expression, in brains from WNV-infected C57Bl/6 mice. During the course of infection skin, spleen and kidney were all sites of WNV replication before virus reached the brain. In brain, increased expression of the chemokines monocyte chemoattractant protein (MCP)-5 (CCL12), interferon gamma inducible protein 10 (IP-10; CXCL10), and monokine induced by gamma interferon (MIG; CXCL9) preceded the expression of interferon gamma (IFN-γ) and tumor necrosis factor alpha (TNF-α), which have previously been considered to be key early cytokines in the pathogenesis and immune response of WNV encephalitis. These results suggest that the chemokines MCP-5, IP-10, and MIG are important triggers of inflammation in brain due to their early up-regulation following WNV infection. *Journal of NeuroVirology* (2007) **13,** 130–138.

Keywords: chemokines; cytokines; histopathology; MCP-5; West Nile virus

Introduction

West Nile virus (WNV) is a member of the Flaviviridae family, genus *Flavivirus*. Other members of this genus include dengue, tick-borne encephalitis, yellow fever, Japanese encephalitis (JEV), Murray Valley encephalitis (MVEV), and St. Louis encephalitis (SLE) viruses. Smithburn and colleagues first isolated WNV in 1937 from the blood of a 37-year-old Ugandan woman in the West Nile District of Northern Uganda at the headwaters of the White Nile (Smithburn *et al*, 1940). Currently WNV is found throughout Africa, Europe, Central Asia, and, most recently, in North America. The first outbreak in the United States was in New York City during the summer of 1999, and the virus subsequently spread across the United States. WNV is transmitted primarily by *Culex* mosquitoes to vertebrate hosts. WNV, like other Flaviviruses, has a positive-stranded RNA genome that codes for three structural proteins and a host-derived lipid envelope. Two lineages of WNV (I and II) have been identified (Lanciotti *et al*, 1999), and recently Bakonayi *et al* (2005) suggested that a third lineage exists in Eastern Europe. All isolates that cause severe human disease fall into lineage I (Bakonayi *et al*, 2005; Suchetana *et al,* 2003).

Because there is no specific treatment for disease caused by WNV, research efforts have focused on diagnosis and prevention. At least two commercial companies have initiated research for development of human vaccines (Monath, 2001). In an attempt to protect horses against WNV, both a formalin-inactivated vaccine and a viral-vectored vaccine have

Address correspondence to Dr. David Garcia-Tapia, Department of Veterinary Pathobiology Department, University of Missouri–Columbia, 1600 E. Rollins Street, Columbia, MO 65211, USA. E-mail: GarciaTapiaD@missouri.edu

Received 4 October 2006; revised 21 November 2006; accepted 15 December 2006.

been developed and are currently in use. Understanding the role of the host immune response in disease pathogenesis is required for development of immune protection with the minimal negative effects. Although the mouse has been used as a reliable model of the *in vivo* infection of WNV, no study has examined the relationship between histopathological changes, viral titers, and the immune response in brain during the course of disease. For the experiment described herein, we use the C57BL/6 strain of mice, a strain that has shown partial resistance to WNV infection and thus has similar rates of mortality to those observed in horses and humans (Charlier *et al*, 2004; Oliphant *et al*, 2005).

To date there is little information about pathological changes observed during the course of WNV infection in the mouse model. Only two reports have provided detailed descriptive information (Chambers and Diamond, 2003; Shrestha, *et al*, 2003). These reports described the kinetics of viral replication, reporting that between 24 and 48 h post infection (p.i.) virus was detectible in blood. By day 4 p.i. virus was isolated in some visceral organs, including spleen and kidney, but no virus was found in liver. At the same time on day 4 p.i., the maximum titers of virus were observed in spleen and kidney, as well as lymph nodes (Chambers and Diamond, 2003). By day 4 p.i. virus was found in brain and spinal cord. Days 9 and 10 p.i. were associated with the highest viral titers in the central nervous system (CNS) (Shrestha *et al*, 2003). There are several reports describing pathological changes found in tissue from infected humans and horses. Most of the reports describe the main features of inflammation in CNS as the presence of perivascular lymphomonocytic infiltrates. The presence of infected neurons in hippocampus, cerebellum, cerebral cortex, brainstem, and ventral horns of spinal cord, as well as the presence of multifocal glial-microglial nodules, neuronal necrosis, and rare neuronophagia have all been described in WNV infection (Agamanolis *et al*, 2003; Cantile *et al*, 2001; Doron *et al*, 2003; Hayes *et al*, 2005; Kelley *et al*, 2003).

Recently Shirato and collaborators reported up-regulation of several chemokines in the brain following WNV infection of mice, including CCL5 (RANTES), CCL3 (macrophage inflammatory protein [MIP]-1α), CCL4 (MIP-1β), and CXCL10 (IP-10) (Shirato *et al*, 2004). The importance of CXCL10 in WNV infection has been demonstrated in mice that lack this chemokine. These animals showed a decrease in the recruitment of CXCR3+CD8+T cells to the brain, an increase in the viral burden in brain, and a higher morbidity and mortality (Klein *et al*, 2005). It has also been reported that the chemokine receptor CCR5 is important in the recruitment of leukocytes into the brain and increases the survival rate to 60% in mice infected with WNV (Glass *et al*, 2005; Lim *et al*, 2006). In a second report, the same research group concluded that a deficiency of this molecule increases the risk of presentation of encephalitis in WNV infections (Glass *et al*, 2006). The expression of CXCL10 and CCL5 has been reported in astrocytes infected *in vitro* by WNV; however, production of tumor necrosis factor alpha (TNF-α) or interferon gamma (IFN-γ) was not detected during the infection (Cheeran *et al*, 2005).

In this study we present a correlation of histopathological events and the expression of chemokines and cytokines in brain following experimental WNV infection of mice, and we propose the potential importance of the chemokine monocyte chemoattractant protein (MCP)-5 (CCL12), along with MIG (CXCL9) and IP-10 (CXCL10), as key initiators of inflammation in the brain during WNV infection. We also describe up-regulation of C10 (CCL6), a novel finding in WNV infection.

Results

Evaluation of histopathology and cytokine expression following WNV infection

Eight-week-old, female C57Bl/6 mice were inoculated with WNV and sacrificed at different time points post infection as described in Material and Methods, in order to evaluate the histopathological changes and correlate those to the expression pattern of chemokines and cytokines in the brain. Table 1 shows the chronology of key pathologic events occurring in the central nervous system following infection. On day 1 p.i. virus was found only in the blood by plaque assay (data not shown), and in skin by immunohistochemistry (IHC) (Figure 1A). Similar findings were obtained on day 2 p.i. By day 4 p.i.

Table 1 Time course of key pathological and viral growth events in brain during infection by West Nile virus

	Day p.i.						
Observation	1	2	4	6	9	13	21
Glial-microglial nodules	0/3	0/3	0/3	2/3	3/3	3/3	0/4
Perivascular infiltration	0/3	0/3	0/3	2/3	3/3	3/3	2/4
Neuronal necrosis	0/3	0/3	0/3	0/3	3/3	1/3	2/4
Neuronophagia	0/3	0/3	0/3	0/3	2/3	1/3	0/4
Satellitosis	0/3	0/3	0/3	2/3	3/3	1/3	2/4
Average viral titer (PFU/g)	N.D.[a]	N.D.	N.D.	$10^{2.78}$	$10^{6.70}$	$10^{3.70}$	N.D.
Virus detected by IHC	0/3	0/3	0/3	2/3	S 3/3	3/3	2/4

[a]N.D., No titers were detected, although titration was attempted.

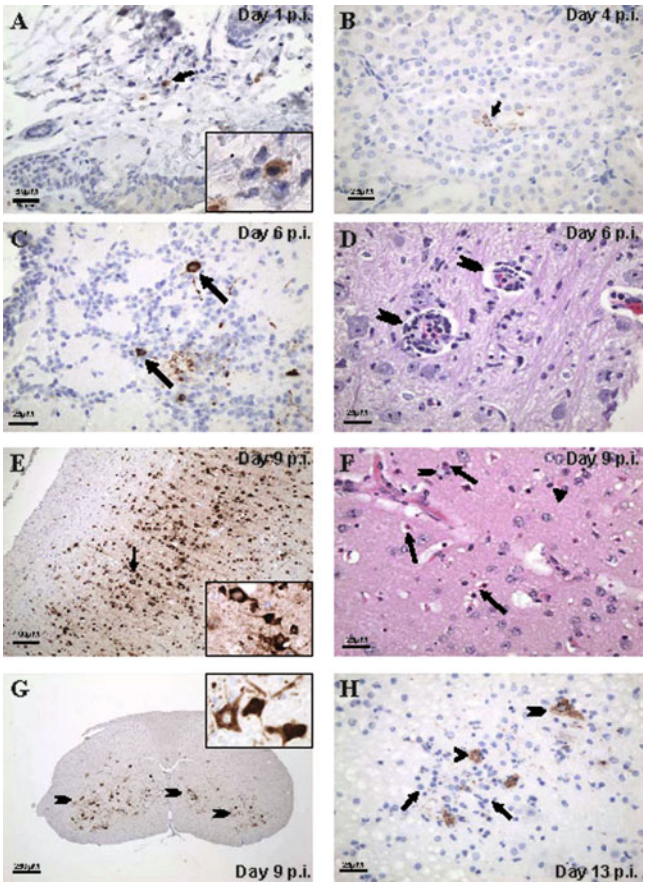

Figure 1 Main features of the pathology of WNV infection in C57Bl/6 mice. (**A**) Detection of WNV antigen by IHC in the cytoplasm of macrophages or dendritic cells present in dermal tissue (arrow in large frame and 10× magnification in the inset). (**B**) Detection of WNV antigen in epithelial cells from renal tubules *(arrow)*. (**C**) Immunodetection of WNV antigen in neurons of the olfactory bulb *(arrows)*. (**D**) An H&E-stained section from brainstem, with moderate perivascular mononuclear infiltrate *(chevron arrows)*. (**E**) A diffuse distribution of intraneuronal WNV antigen in cerebral cortex *(arrow)*, the small frame is 4× magnification from one of the affected areas, with cytoplasmic localization of WNV antigen. (**F**) An H&E-stained section from the same area of cerebral cortex presented in **E**. A severe diffuse neuronal necrosis is observed, which is characterized by shrunken neurons with highly eosinophilic cytoplasm and pyknotic nucleus *(arrows)*. Foamy macrophages approaching to a necrotic neuron (neuronophagia pointed with a chevron arrow), and gliosis *(arrowhead)* are also observed. (**G**) Immunolocalization of WNV antigen in neurons of the ventral horns of spinal cord *(chevron arrows)*, the inset frame is a 10× magnification of the large frame, showing the localization of virus in cytoplasm and neurites. (**H**) A section of spinal cord with neurons containing virus *(chevron arrow)* and multifocal glial-microglial nodules *(arrow)* surrounding accumulations of WNV antigen, which apparently is contained inside necrotic neurons *(arrowheads)*.

the mice were still viremic and for the first time WNV was detected in both spleen and kidney by plaque assay (data not shown), and by IHC (Figure 1B). On this day, a faint up-regulation of the chemokine MCP-5 was detected in brain (Figure 2C).

Day 6 p.i. was the first day in which the virus was detectable in brain, and this was also the day in which glial-microglial nodules, satellitosis (defined as neurons surrounded by microglial cells and macrophages), and perivascular mononuclear infiltrates were observed in two out from three animals (Table 1). The maximum titers obtained from this organ were approximately $10^{3.60}$ plaque-forming units (PFU)/g with an average of $10^{2.78}$ PFU/g (Figure 2A). Immunohistochemical staining demonstrated that macrophages and fibrocytes of the skin were positive for WNV. Few macrophages were detected as positive for WNV in spleen and some epithelial tubular cells of kidney contain viral antigen (data not shown). Although the virus was detected in these three organs, no signs of inflammation were observed. Consistent with results from viral titrations, IHC detection of WNV was positive for the first time on day 6 p.i. in the brain, in which there were multifocal areas with some neurons from the olfactory bulb that stained positive for WNV (Figure 1C). The virus was also detected in spinal cord, brainstem, and cerebral cortex, where small foci of neurons were positive by IHC for WNV. Moderate multifocal mononuclear perivascular infiltrates (Figure 1D), as well as moderate multifocal gliosis and neuronal satellitosis were observed in brainstem and spinal cord. At the same time a clear up-regulation of the chemokines MCP-5 (CCL12), IP10 (CXCL10), MIG (CXCL9), as well as a slight up-regulation of MCP-1 (CCL2), were detected in at least one out of three mice sacrificed on day 6 p.i. (Fig. 2A and C). For the first time following infection, neutralizing antibodies were detected with titers up to 1:20 (Fig. 2C). Immunoglobulin M (IgM) was the predominant isotype detected by IFA (data not shown).

Day 9 p.i. may be considered the most critical day in the course of the experiment, given that the most severe lesions and the highest viral titers in brain were observed on this day. In addition, this was the time point in which mice began showing clinical signs and the more severely affected animals died on this day. In the second experiment, day 9 p.i. was the day in which all the mortality was observed (Figure 3). Once the clinical signs, characterized by the appearance of a rough hair coat, lethargy, apathy, incoordination, segregation from the group, difficulty in swallowing, and prostration were observed, the animals died in less than 12 h. Viral titers in brain were the highest observed in all the tissues analyzed, reaching $10^{7.9}$ PFU/g (mean = $10^{6.4}$ PFU/g). The virus was still detected in kidney and spleen. Although the viral concentrations were very high in the brain, no virus was detected in blood on day 9 p.i.

On day 9 p.i., all the animals presented with inflammatory lesions in the cerebral cortex, hippocampus, brainstem and spinal cord. A summary of the events that occurred on this day are presented in Table 1. The inflammation was characterized by multifocal perivascular mononuclear infiltrates, composed mainly of macrophages and lymphocytes with scant neutrophil infiltration and neuronal necrosis

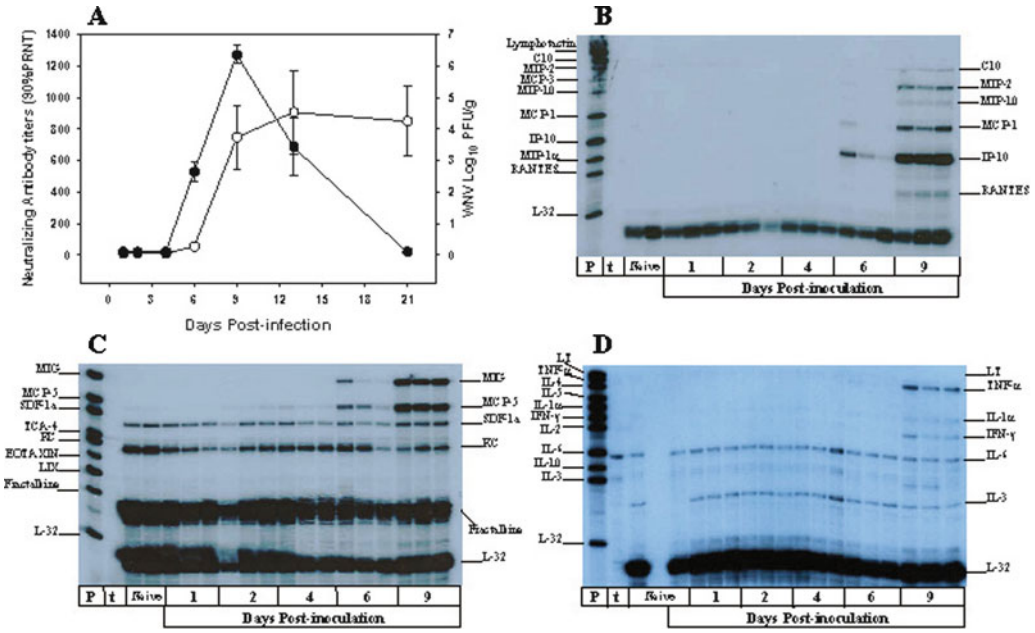

Figure 2 Kinetics of viral replication, neutralizing antibody production, and chemokine and cytokine expression during an infection by WNV in C57Bl/6 mice. (**A**) Neutralizing antibody production curve (*open symbols*, *y* left axis) and the viral growth curve in brain (*closed symbols, y* right axis), in mice infected with WNV. Values are the mean antibody titers or viral ± SEM of triplicates from one representative experiment. (**B–D**) RNase protection assay results performed using RNA samples from the brain of WNV-infected mice. Detection of chemokine expression was performed on days 1, 2, 4, 6, and 9. Three mice per group were euthanized on the indicated days. t, a transfer RNA control. Naïve controls were uninfected mice sacrificed on day 1 or 4 of the experimental time course. P, molecular probe control. The chemokines (**B** and **C**) or cytokines (**D**) analyzed are listed on the left axis of each gel.

with multifocal gliosis and satellitosis (Figure 1F). In the spinal cord extensive localization of the virus by IHC was detected mainly in the ventral horns (Figure 1G), although in one mouse the dorsal horns were also partially affected. A few neurons from the hippocampus, cerebral cortex, and brainstem stained positive for WNV in a multifocal pattern. In the more clinically ill mice, the lesions were more severe. In these animals, an extensive area of the cerebral cortex stained positive for WNV by IHC. The virus was identified in neuronal cytoplasm, axons, and dendrites (Figure 1E). Additionally there were areas with multifocal positive staining of neurons and astrocytes in the spinal cord, brainstem, hippocampus, and cerebellum in which the affected cells were the granular cells with only a few stellate neurons infected. In these mice neuronal necrosis was evident in the cerebral cortex and an extensive area of WNV antigen was detected by IHC in the cytoplasm of necrotic neurons. Those neurons were shrunken and had eosinophilic cytoplasm with pyknotic or karyorrhectic nucleus, and some of the neurons were surrounded by microglia cells and lymphocytes (Figure 1F). Neuronophagia (Figure 1F) was also observed in the affected areas from two animals (Table 1), and perivascular infiltrates were present with disruption of the endothelium in some vessels and moderate hemorrhage. In mice that were euthanized due to a moribund condition, the spleen was severely depleted, and the thymus was also affected by lymphoid depletion, which was characterized by abundant numbers of lymphocytes with karyorrhectic or pyknotic nuclei.

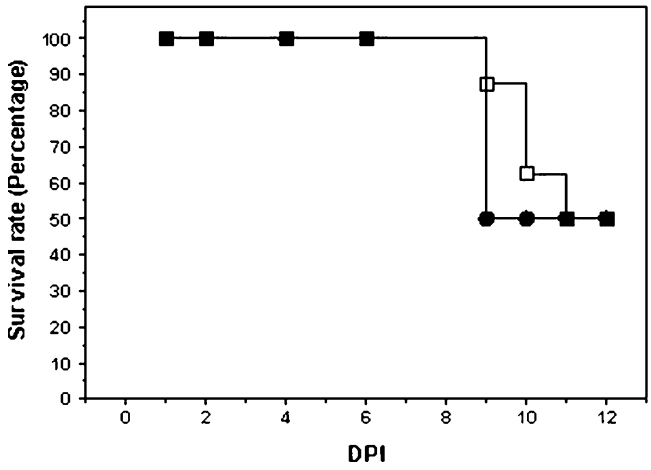

Figure 3 Mortality in mice infected with West Nile virus in two different experiments. Percentage of surviving animals during a WNV infection obtained from two independent experiments is presented. The mice were inoculated subcutaneously with 100 PFU of WNV. The time points indicate the percentage of surviving animals at the point of reference.

In the brain of mice sacrificed on day 9 p.i., significant up-regulation of several cytokines and chemokines was detected. In all the brains analyzed, TNF-α, interleukin (IL)-1α, IFN-γ, and the

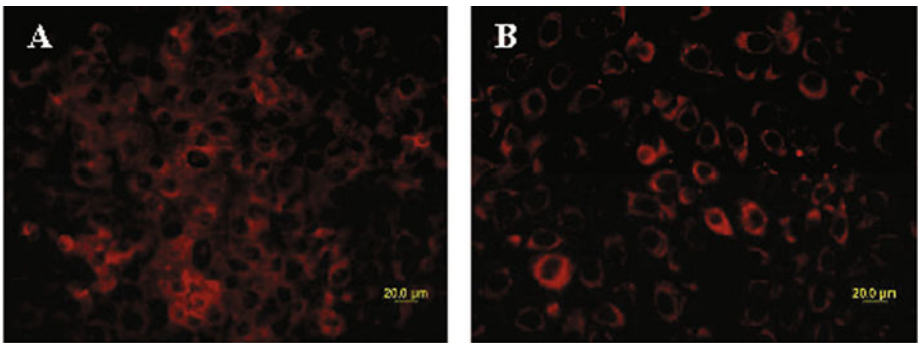

Figure 4 Detection of specific anti-WNV antibodies in infected C57Bl/6 mice. Identification of IgM (**A**) and IgG (**B**) in serum from WNV-infected mice sacrificed on day 9 p.i. Identification of antibodies was performed by IFAT using mouse serum diluted 1:10 as primary antibody and goat anti-mouse IgM or IgG conjugated to rhodamine as secondary antibodies.

immunomodulatory cytokine transforming growth factor (TGF)-ß1 were up-regulated, whereas the chemokine C10 (CCL6) was detected for first time in the infected mice, as well as MIP-2 (CXCL2) , MIP-1ß (CCL4), and RANTES (CCL5). The chemokines up-regulated on day 6 p.i. showed increased expression on day 9 p.i., leading to clear detection of the transcript for MCP-5 (CCL12), IP-10 (CXCL10), MIG (CXCL9), and MCP-1 (CCL2) (Figure 2B, C, and D). The titer of neutralizing antibodies was clearly increased on this day, reaching titers of up to 1:900 with an average of 1:700 (Figure 2A). On day 9 p.i., specific anti-WNV IgM and IgG antibodies were clearly identified in the serum of infected mice by using immunofluorescense antibody test (IFA) (Figure 4A and B).

Day 11 p.i. was the last day in which mortality was observed. On day 13 p.i., viral titers were still detected in several organs such as the brain, which had titers up to 10^7 PFU/g. Virus was also detected in lymph nodes (10^5 PFU/g) from one out of three mice sacrificed on this day. The kidney and spleen from two mice had viral titers of approximately 1000 PFU/g and 100 PFU/g, respectively. No virus was detected in blood on this day.

Multifocal staining of infected neurons was detected by IHC for WNV in the spinal cord, hippocampus, and cerebral cortex. In addition, there was still evidence of inflammatory lesions in the brainstem, cerebral cortex, hippocampus, and spinal cord. At day 13 p.i., three out of three mice had multifocal glial-microglial nodules, mainly in brainstem and spinal cord (Table 1 and Figure 1H). In one of three mice evaluated, neuronal necrosis and satellitosis were observed in the cerebral cortex and brainstem, as well as neuronophagia in the ventral horns of spinal cord. Perivascular mononuclear infiltrates and glial-microglial nodules were observed in all the animals (Table 1). In spleen and thymus, moderate to severe depletion of lymphoid tissue was observed. The neutralizing antibody titers continued to increased, with a maximum observed titer of 1:1260 (mean = 1:900). On day 21 p.i., no virus was detected in any tissue by plaque assay. In two of four mice examined, multifocal satellitosis and scattered small nodules of microglia cells were located close to necrotic neurons that were positive for WNV by IHC. These changes were observed mainly in cerebral cortex, brainstem and spinal cord (Table 1).

Discussion

Consistent with previous reports, blood was the only sample on day 1 p.i. in which WNV was detected following experimental infection of mice (Diamond *et al*, 2003; Kramer and Bernard, 2001). Additionally, in our analyses WNV was also identified in skin by IHC from day 1 though day 4 p.i. No previous report exists describing detection or replication of WNV in skin, other than that of Johnston *et al* (2000), which suggested that after peripheral inoculation WNV was able to infect Langerhans' dendritic cells, which subsequently migrate to draining lymph nodes were viral replication has been observed in other studies (Diamond *et al*, 2003a; McMinn *et al*, 1996). Prior reports indicate that day 4 p.i. is the time of the peak viral replication in spleen and kidney (Diamond *et al*, 2003; Kramer and Bernard, 2001; Xiao *et al*, 2001), as we have found in our experiments. On this day, we also detected WNV by IHC in the cytoplasm of renal tubular epithelial cells. This finding supports the previous result by Buckweitz *et al* (2003) in which antigens of WNV were detected in renal tubules from an infected dog.

Several pathological lesions have been reported to occur in CNS after infection with WNV in mice (Diamond *et al*, 2003; Hunsperger and Roehrig, 2006), humans, and horses (Agamanolis *et al*, 2003; Cantile *et al*, 2001; Doron *et al*, 2003; Hayes *et al*, 2005; Kelley *et al*, 2003). Those findings include the infection of neurons in ventral horns of spinal cord, olfactory bulb, hippocampus, brainstem, and cerebellum; as well as the development of perivascular mononuclear infiltrates, glial-microglial nodules, neuronal degeneration, neuronal death, satellitosis, and neuronophagia. Our results are consistent with those previous reports, with localization of WNV

antigen in neuronal cytoplasm and neurites of the above mentioned anatomic areas of the CNS, plus the occurrence of all the inflammatory changes reported previously.

Mice that had not died or were not euthanized (due to moribund condition) by day 13 p.i. were considered survivors from the infection. WNV was still detected in CNS of these mice, suggesting a potential persistent infection. Persistent viral infection has been reported to occur in other flaviviral infections (Chambers and Diamond, 2003). The host immune response, together with some properties of the neuronal environment, allow the possibility of persistence, and both may contribute to the presentation of phenotypic variation in the persistent viruses. An example is the attenuation of WNV, which was persistent in monkeys (Pogodina *et al*, 1983); however, the persistence of Sindbis virus infection in mice led to the emergence of neurovirulent strains (Levin and Griffin, 1993).

TNF-α plays a pivotal role in the immunity and pathogenesis of viral encephalitis and it has been demonstrated that in an infection caused by Murray encephalitis virus. This molecule acts in two different ways: (1) activating neurovascular endothelium and increasing adhesion molecule expression, and (2) attracting neutrophils via induction of the neutrophil attracting chemokine N51/KC (CXCL1) (King *et al*, 2003). Recently Wang and collaborators (2004) demonstrated that in the absence of Toll-like receptor (TLR)-3, WNV titers were increased in blood but were reduced in the CNS. Additionally, neuropathology was diminished and mortality also reduced during WNV infection (Wang *et al*, 2004). From these results, the authors suggested that TLR-3 played a role the movement of WNV across the blood-brain barrier, especially because cross-linking of this receptor up-regulated expression of TNF-α, which in turn increased capillary permeability by stimulation of the endothelial cells in the brain blood capillaries (Diamond and Klein, 2004). In a similar manner, IFN-γ has been reported to be important for induction of lymphotactic chemokines such as IP-10 (CXCL10), thereby influencing the movement of T cells into the brain parenchyma (Dufour *et al*, 2002). Our results showed an up-regulation of TNF-α and IFN-γ, although these two molecules were not up-regulated until day 9 p.i. This up-regulation was detected after up-regulation of other chemokines such as MCP-5 (CCL12), IP-10 (CXCL10), and MIG (CXCL9), which were clearly up-regulated or expressed on day 6 p.i. The production of IP-10 in brain has been attributed to perivascular glial cells, perivascular astrocytes, and endothelial cells (Prat *et al*, 2001). It has also been reported that IP-10 is produced in early stages of *in vitro* infection of microglial cells and astrocytes by WNV (Cheeran *et al*, 2005). MCP-5 has been demonstrated to be a potent monocyte chemoattractant produced in part by endothelial cells (Sarafi *et al*, 1997). Day 6 p.i. was also the first day in which a perivascular infiltrate was observed in infected mice. Even though other murine models have suggested TNF-α and IFN-γ as important factors in the pathogenesis of WNV encephalitis, our results demonstrate that those molecules may have a role after some other molecules triggered the inflammatory process in brain. Our hypothesis is that IP-10 and MCP-5 initiate recruitment of leukocytes into perivascular spaces. Here antigen presentation occurs, which leads to activation of circulating leukocytes that produce IFN-γ, IL-1α, and TNF-α. These molecules increase the permeability of brain capillaries and facilitate entry of inflammatory cells into the brain parenchyma, helping eliminate the virus in CNS. It is possible that these events also facilitate entry of infected monocytes, thereby increasing the viral burdens and neuronal infection of brain.

Klein and collaborators demonstrated the importance of IP-10 in protection against WNV encephalitis by using mice deficient in CXCL10 (IP-10). These mice developed higher burdens of virus in brain, as well as presented with more severe pathology and experienced enhanced morbidity and mortality when compared to WNV inoculated wild-type mice (Klein *et al*, 2005). The authors suggest that this molecule may be neuroprotective in response to WNV infection in the CNS. However, based on our results, the production of this molecule along with other chemokines as MCP-5 and MIG indicates that IP-10 may have an important role in the induction of strong inflammation in the brain, and therefore could play a role in the pathogenesis of encephalitis caused by WNV, more than in the clearance of the virus. Recent publications reported the up-regulation of other chemokines during WNV encephalitis. The chemokines that have been reported to be up-regulated during a murine infection by WNV are CXCL10 (discussed above), CXCL9 (MIG), CXCL2 (MIP-2), CCL2 (MCP-1), CCL3 (MIP-1α), CCL4 (MIP-1β), CCL5 (RANTES), and CCL7 (MCP-3) (Glass *et al*, 2005; Klein *et al*, 2005). Expression of these chemokines was detected on days 6 and 9 p.i. in this study. Differing from previous reports, we found earlier up-regulation (day 4 p.i.) of MCP-5 (CCL12) and later up-regulation of C10 (CCL6) on day 9 p.i. MCP-5 (CCL12) is a chemokine that has been suggested as an important player in the initiation of autoimmune inflammation in the brain after cortical injury in a murine model of autoimmune encephalomyelitis (Sun *et al*, 2000). Our results support this possibility due to the early up-regulation of the chemokine MCP-5 observed during a WNV infection, which suggests a potential role of MCP-5 as initiator of inflammation in the brain of WNV- infected mice. CCL6 is a chemokine that has been identified to be produced by microglial cells. It is thought to be important in cell-to-cell communication and is induced by IFN-γ, whereas TNF-α has no effect on its regulation (Kanno *et al*, 2005). Asensio *et al* (1999) described this molecule as a prominent chemokine expressed

in CNS during demyelinating disease, inducing the recruitment of macrophages and CD4+ T cells into the brain parenchyma.

In summary, our results suggest that MCP-5, IP-10, and MIG are key early molecules in triggering the inflammatory CNS events following WNV infection. Up-regulation of MCP-5 (CCL12) and C10 (CCL6) was observed for the first time in a murine infection by WNV, suggesting that along with IP10 (CXCL10), MIG (CXCL9), MCP-1 (CCL2), MIP-1α (CCL3), MIP-1ß (CCL4), RANTES (CCL5), and MCP-3 (CCL7), these molecules play an important role inducing a potent cellular helper T cell (Th)-1 type immune response against WNV in the CNS.

Material and methods

Virus and cell culture

An isolate of WNV (Garcia-Tapia *et al*, 2006) was propagated in Vero cell cultures using standard techniques (Burleson *et al*, 1992). Vero cell cultures were maintained in Dulbecco's modified Eagle medium (DMEM) supplemented with 10% heat-inactivated fetal bovine serum (FBS) and 2 mM L-glutamine, 0.25 μg/ml fungizone, and 0.5 mg/ml gentamycin (cell culture reagents supplied by Mediatech, Herndon, VA). The cells were maintained at 37°C in a humidified 5% CO_2 incubator. Quantification of WNV stocks and experimental samples (homogenized tissues from infected mice) was performed using a viral plaque assay. Tenfold serial dilutions of samples were adsorbed for 2 h onto confluent Vero cell monolayers in 6-well plates (10 cm^2/well). Cell monolayers were washed once with cell culture medium. Overlay medium, which consisted of maintenance medium plus 0.5% (*w*/*v*) agarose, was then added to each well. Cultures were maintained at 37°C in a humidified 5% CO_2 incubator for 3 days. Overlays were then removed and cell monolayers were stained with 0.5% (*w*/*v*) crystal violet/70% (*v*/*v*) methanol and plaques were counted and viral titers were calculated (Burleson *et al*, 1992).

Mice

Specific pathogen–free, 7- to 8 week-old C57BL/6 female mice (Jackson Labs, NJ, USA) were maintained in biosafety level 3 (BSL-3) facilities and housed in microisolator cages. Water and feed were provided *ad libitum*. All experiments were performed in compliance with the Animal Welfare Act and other regulations relating to animals and experiments involving animals and in adherence to the *Guide for Care and Handling of Laboratory Animals of the University of Missouri* (protocol number 4038).

Experimental design

Two independent experiments were conducted using C57Bl/6 mice, which were inoculated with 100 PFU of WNV in the footpad through subcutaneous inoculation (100 μl). The experiment 1 was performed using 25 animals, with 3 mice euthanized on days 1, 2, 4, 6, 9, 13 and 21 p.i. On days 1 and 4 p.i., uninfected control mice were also euthanized. Eighteen mice were used for experiment 2, with three mice euthanized on days 1, 2, 4, 6, 9, and 13 p.i. On days 1 and 4 three uninfected mice were euthanized. In both experiments, the mice that showed clinical signs of encephalitis were euthanized at the time when severe signs were observed. Samples of blood, spleen, liver, kidney, lymph node, and brain were taken for viral titration, and RNase protection assays (RPAs); these same organs plus skin, pancreas, lung, heart, thymus, adrenal glands, and muscle were collected for histopathology (HP) and immunohistochemistry (IHC) studies.

Tissue homogenization

Blood, spleen, liver, kidney, lymph node, and brain were collected at necropsy and placed in previously frozen plastic vials containing zirconia-silica beads (catalog number 11079110z; Biospec Products, Bartlesville, OK). The vials containing the tissue were immediately immersed in liquid nitrogen then transferred to −80°C where they were held until homogenization. To homogenize tissues, 1 ml of DMEM (supplemented with 10% fetal bovine serum) or TRIzol (catalog number 15596-018; Invitrogen, Carlsbad, CA) was added to each vial. The vials were then subjected to agitation in a mini bead-beater-8 (Biospec Products) for 2 min. The samples were then processed for viral titration by plaque assay or RNA was extracted for analysis by RNase protection assays (RPAs).

RNA extraction and RPA

Total RNA was extracted using TRIzol reagent (catalog number 15596-018; Invitrogen) according to the manufacturer's instructions. RNA concentrations were determined by ultraviolet (UV) spectroscopy at 260 nm. The RPA was performed by a previously described method (Asensio and Campbell, 1997). For the synthesis of a radiolabeled antisense RNA probe set for chemokines and the loading control RPL32, the final reaction mixture (10 ml) contained 120 mCi of [α-^{32}P]UTP (3000 Ci/mmol; Andotek, Irvine, Calif.), UTP (73 pmol), GTP, ATP, and CTP (2.5 mmol each), dithiothreitol (DTT) (100 nmol), transcription buffer, RNase inhibitor (20 U; Ambion), T7 polymerase (10 U; Promega), and an equimolar pool of *Eco*RI-linearized templates (15 ng each). After 1 h at 37°C, the mixture was treated with DNase I (2 U; Ambion) for 30 min at 37°C and the probe was purified by extraction with phenol-chloroform and precipitated with ethanol. Dried probe was then dissolved (2.63×10^5 dpm/ml) in hybridization buffer [80% formamide–0.4 M NaCl–1 mM EDTA–40 mM piperazine-*N*,*N*^{9}-bis(2-ethanesulfonic acid) (PIPES) (pH 6.4)], and 10 ml of this mixture was added to tubes containing target RNA dissolved in Tris-EDTA buffer (TE). The samples were overlaid with mineral

oil, heated to 95°C, and then incubated at 56°C for 12 to 16 h. Single-stranded RNA was digested for 45 min at 30°C by the addition of a mixture of RNase A (0.2 mg/ml) and RNase T1 (50 U/ml; Promega) in 10 mM Tris (pH 7.5)–300 mM NaCl–5 mM EDTA (pH 8). After incubation, 18 ml of a mixture containing proteinase K (1.5 mg/ml; Boehringer Mannheim, Indianapolis, IN), sodium dodecyl sulfate (3.5%), and yeast tRNA (200 mg/ml; Sigma) was added, and the samples were incubated for 30 more min at 37°C. The RNA duplexes were isolated by extraction and precipitation as described above, dissolved in 80% formamide and dyes, and electrophoresed in a standard 6% acrylamide–7M urea–0.5% Tris-borate-EDTA sequencing gel. Dried gels were placed on XAR film (Kodak, Rochester, NY) with intensifying screens and exposed at 270°C. Probe sets used throughout this study included the cytokine probe sets ML11 and ML26, and the chemokine probe sets 1 and 2 (CS1, CS2) (Asensio and Campbell, 1997).

Plaque-reduction neutralization assays

The plaque-reduction neutralization titers (PRNTs) of serum from mice were determined by adding 50 plaque-forming units of WNV to serial twofold dilutions of heat-inactivated (56°C, 30 min) mouse serum. Samples were incubated at 37°C for 1 h, followed by 1 additional hour at room temperature prior to adsorption to confluent Vero cell monolayers. After adsorption for 2 h, the inoculum was removed and the monolayer was rinsed once with cell culture medium and then replaced with cell culture medium containing 0.5% (*w*/*v*) agarose. Three to 4 days following inoculation, the agarose overlay was removed and cell monolayers were stained as described above. Viral plaques were counted and the PRNT was recorded as the final serum dilution that reduced the number of plaques by ≥90% compared to control wells, to which no horse serum had been added.

Histology and immunohistochemistry

Tissue samples were fixed in 10% formalin, then trimmed and embedded in paraffin, sectioned (5 μm thickness), and mounted on positively charged glass slides. The tissue sections were stained with hematoxilin and eosin for histopathological examination. For IHC, a polyclonal anti-WNV antibody derived from rabbit was used (catalog number C-585, Invitrogen-Bioreliance, Carlsbad, CA). The antibody was adsorbed against normal mouse tissue for 2 h at 37°C and then centrifuged at 16,000 × *g* for 30 min at 10°C and used for IHC. The preadsorbed antibody was used as primary antibody at a final dilution of 1:800 in antibody dilution buffer (Dako Cytomation, Carpinteria, CA). The Dako EnVision System (DAKO Cytomation) was used as an amplification and reporter system. The assay was partially performed in a Dako Autostainer Universal Staining System. Briefly, tissue sections were deparaffinized and rehydrated. To increase staining intensity, an antigen retrieval procedure with steaming of the samples was used. Endogenous peroxidases were blocked by incubation in 0.03% hydrogen peroxide. Tissue sections were incubated with a 1:800 dilution of primary antibody, followed by the secondary antibody (horseradish peroxidase–labeled polymer conjugated to goat anti-rabbit total immunoglobulin). Staining was completed by adding the substrate-chromogen diaminobenzidine (DAB). All samples were incubated in a humidified chamber at room temperature (25°C to 27°C). Tissues were counterstained with hematoxylin, dehydrated, and cleared, then coverslips were applied. Negative controls were performed by substitution of normal rabbit serum for the primary antibody, as well as the incubation of the preadsorbed antibody with normal mouse tissues. Sections of confirmed WNV positive mouse tissue were uses as positive controls, as well as WNV-positive avian tissue.

References

Agamanolis DP, Leslie MJ, Caveny EA, Guarner J, Shieh WJ, Zaki SR (2003). Neuropthological findings in West Nile virus encephalitis. A case report. *Ann Neurol* **54:** 547–551.

Asensio VC, Campbell IL (1997). Chemokine gene expression in the brains of mice with lymphocytic choriomeningitis. *J Virol* **71:** 7832–7840.

Asensio VC, Lassmann S, Pagenstecher A, Steffensen SC, Henriksen SJ, Campbell IL (1999). C10 is a novel chemokine expressed in experimental inflammatory demyelinating disorders that promotes recruitment of macrophages to the central nervous system. *Am J Pathol* **154:** 1181–1191.

Bakonyi T, Hubalek Z, Rudolf I, Nowotny N (2005). Novel Flavivirus or new lineage of West Nile virus, Central Europe. *Emerg Infect Dis* **11:** 225–231.

Buckweitz S, Kleiboeker S, Marioni K, Ramos-Vara J, Rottinghaus A, Schwabenton B, Jonson G (2003). Serological, reverse transcriptase-polymerase chain reaction, and immunohistochemical detection of West Nile virus in a clinically affected dog. *J Vet Diagn Invest* **15:** 324–329.

Burleson FG, Chambers TM, Wiedbrauk DL (1992). *Virology: A laboratory manual* San Diego, CA: Academic Press, pp 74–84.

Cantile C, Del Piero F, Di Guardo G, Arispici M (2001). Pathologic and immunohistochemical findings in naturally occuring West Nile virus infection in horses. *Vet Pathol* **38:** 414–421.

Chambers TJ, Diamond MS (2003). Pathogenesis of flavivirus encephalitis. *Adv Virus Res* **60:** 273–342.

Charlier N, Leyssen P, De Clercq E, Neyts J (2004). Rodent models for the study of therapy against flavivirus infections. *Antiviral Res* **63:** 67–77.

Cheeran MCJ, Hu S, Sheng WS, Rashid A, Peterson PK, Lokensgard JM (2005). Differential responses of human

brain cells to West Nile virus infection. *J NeuroVirol* **11:** 512–524.

Diamond MS, Klein RS (2004). West Nile virus: crossing the blood-brain barrier. *Nat Med* **10:** 1294–1295.

Diamond MS, Shrestha B, Marri A, Mahan D, Engle M (2003). B cells and antibody play critical roles in the immediate defense of disseminated infection by West Nile encephalitis virus. *J Virol* **77:** 2578–2586.

Dufour JH, Dziejman M, Liu MT, Leung JH, Lane TE, Luster AD (2002). IFN-γ-inducible protein 10 (IP-10; CXCL10)-deficient mice reveal a role for IP-10 in effector T cell generation and trafficking. *J Immunol* **168:** 3195–3204.

Doron SI, Dashe JF, Adelman LS, Brown WF, Werner BG, Hadley S (2003). Histopathologically proven poliomyelitis with quadriplegia and loss of brainstem function due to West Nile virus infection. *Clin Infect Dis* **37:** e74–e77.

Garcia-Tapia D, Loiacono CM, Kleiboeker SB (2006). Replication of West Nile virus in primary equine peripheral blood mononuclear cell cultures. *Vet Immunol Immunopathol* **110:** 229–244.

Glass WG, Lim JK, Cholera R, Pletnev AG, Gao JL, Murphy PM (2005). Chemokine recptor CCR5 promotes leukocyte trafficking to the brain and survival in West Nile virus infection. *J Exp Med* **202:** 1087–1098.

Glass WG, McDermott DH, Lim JK, Leghong S, Fong Yu S, Frank WA, Pape J, Cheshier RC, Murphy PM (2006). CCR5 deficiency increases risk of symptomatic West Nile virus infection. *J Exp Med* **203:** 35–40.

Hayes EB, Komar N, Nasci RS, Montgomery SP, O'Leary DR, Campbell GL (2005). Epidemiology and transmission dynamics of West Nile virus disease. *Emerg Infect Dis* **11:** 1167–1173.

Hunsperger EA, Roehrig JT (2006). Temporal analyses of the neuropathogenesis of a West Nile virus infection in mice. *J NeuroVirol* **12:** 129–139.

Johnson DJ, Ostlund EN, Pedersen DD, Schmitt BJ (2001). Detection of North American West Nile virus in animal tissue by a reverse transcription-nested polymerase chain reaction assay. *Emerg Infect Dis* **7:** 739–741.

Johnston J, Halliday GM, King NJC (2000). Langerhans cells migrate to local lymph nodes following cutaneous infection with an arbovirus. *J Invest Dermatol* **114:** 560–568.

Kanno M, Suzuki S, Fujiwara T, Yokoyama A, Skamoto A, Takahashi H, Imai Y, Takanaka J (2005). Functional expression of CCL6 by rat microglia: a possible role of CCL6 in cell-cell communication. *J Neuroimmunol* **167:** 72–80.

Kelley TW, Prayson RA, Ruiz AI, Isada CM, Gordon SM (2003). The neuropathology of West Nile virus meningoencephalitis and report of two cases and review of literature. *Am J Clin Pathol* **119:** 749–753.

King NJC, Shrestha B, Kesson AM (2003). Immune modulation by Flaviviruses. *Adv Virus Res* **60:** 121–155.

Klein RS, Lin E, Zhang B, Luster AD, Tollet J, Samuel MA, Engle M, Diamond MS (2005). Neuronal CXCL10 directs CD8+ T-cell recruitment and control of West Nile virus encephalitis. *J Virol* **79:** 11457–11466.

Kramer LD, Bernard KA (2001). West Nile virus infection in birds and mammals. *Ann N Y Acad Sci* **951:** 84–93.

Lanciotti RS, Roehrig JT, Deubel V, Smith J, Parker M, Steele K, Crise B, Volpe KE, Crabtree MB, Scherret JH, Hall RA, MacKenzie JS, Cropp CB, Panigrahy B, Ostlund E, Schmitt B, Malkinson M, Banet C, Weissman J, Komar N, Savage HM, Stone W, McNamara T, Gubler DJ (1999). Origin of the West Nile virus responsible for an outbreak of encephalitis in the Northeaster United States. *Science* **286:** 2333–2337.

Levine B, Griffin DE (1993). Molecular analysis of neurovirulent strains of Sindbis virus that evolve during persistent infection of scid mice. *J Virol* **67:** 6872–6875.

Lim JK, Glass WG, McDermott DH, Murphy PM (2006). CCR5: no longer a "good for nothing" gene-chemokine control of West Nile virus infection. *Trends Immunol* **27:** 308–312.

McMinn PC, Dalgrano L, Weir RC (1996). A comparison of the spread of Murray Valley encephalitis viruses of high or low neuroninvasiveness in tissues of Suiss mice after peripheral inoculation. *Virology* **220:** 414–423.

Monath TP (2001). Prospects for developing of a vaccine against the West Nile Virus. *Ann N Y Acad Sci* **951:** 1–12. Review.

Oliphant T, Engle M, Nybakken GE, Doane C, Johson S, Huang L, Gorlatov S, Mehlhop E, Marri A, Chung KM, Ebel GD, Kramer LD, Fremont DH, Diamond MS (2005). Development of a humanized monoclonal antibody with therapeutic potential against West Nile virus. *Nat Med* **11:** 522–530.

Pogodina VV, Frolova MP, Malenko GV, Fokina GI, Koreshkova GV, Kiseleva LL, Bochkova NG, Ralph NM (1983). Study on West Nile virus persisitence in monkeys. *Arch Virol* **75:** 71–86.

Prat A, Biernacki K, Wosik K, Antel JP (2001). Glial cell influence on the human blood brain barrier. *Glia* **36:** 145–155.

Sarafi MN, Garcia-Zepeda EA, McLean JA, Charo IF, Luster A (1997). Murine monocyte chemoattractant protein (MCP)-5: A novel CC chemokine that is a structural and functional homologue of human MCP-1. *J Exp Med* **185:** 99–109.

Shirato K, Kimura T, Mizutani T, Kariwa H, Takashima I (2004). Different chemokine expression in lethal and non-lethal murine West Nile virus infection. *J Med Virol* **74:** 507–513.

Shrestha B, Gottlieb D, Diamond M (2003). Infection and injury of neurons by West Nile encephalitis virus. *J Virol* **77:** 13203–13213.

Smithburn KC, Hughes TP, Burke AW, Paul JH (1940). A neurotropic virus isolated from the blood of a native of Uganda. *Am J Trop Med* **20:** 471–492.

Suchetana M, Bong-Suk K, Chipman PR, Rossmann MG, Kuhn RJ (2003). Structure of West Nile Virus. *Science* **10:** 302.

Sun D, Tani M, Newman TA, Krivacic K, Phillips M, Chernovsky A, Gill P, Wei T, Griswould KJ, Ransohoff RM, Weller RO (2000). Role of chemokines, neuronal projections, and the blood-barrier in the enhancement of cerebral EAE following focal brain damage. *J Neuropathol Exp Neurol* **59:** 1031–1043.

Wang T, Town T, Alexopoulou L, Anderson JF, Fikrig E, Flavell RA (2004). Toll-like receptor 3 mediates West Nile virus entry into the brain causing lethal encephalitis. *Nat Med* **10:** 1366–1373.

Xiao SY, Guzman H, Zhang H, Travassos da Rosa AP, Tesh RB (2001). West Nile virus infection in the golden hamster (*Mesocricetus auratus*): a model for West Nile encephalitis. *Emerg Infect Dis* **7:** 714–721.